

Comparison of EPOS and QGSJET-II in EAS Simulation using CORSIKA code

Chabin Ch. Thakuria, and K. Boruah

Abstract—In this work we compare the predictions of two representative hadronic interaction models, EPOS 1.99, and QGSJET II-03 with several extensive air showers (EAS) parameters for proton and iron primaries in the energy range $10^{17} - 10^{19} \text{ eV}$ using CORSIKA-6990. The EAS parameters depth of shower maximum, shower size, size of muon shower, muon number distribution, electron number distribution, size of hadron shower, hadron energy sum, electron muon correlations, and, hadron energy spectra are studied in this paper.

Index Terms—hadronic interaction models, EAS, X_{max}

I. INTRODUCTION

WHEN high-energy cosmic rays enter into the Earth's atmosphere they initiate cascades of secondary particles producing extensive air showers (EAS). Information regarding the shower generating primary particle have to be derived from the registered information of secondary particles at observation level. The interpretation of properties of primary radiation derived from air shower measurements depends on the understanding of the complex processes of high-energy interactions during the development of air showers. From the number and distribution of various ground particles of the EAS, the reconstruction of energy and the mass of the primary particle can be done. But to relate the observables to primary energy and mass, more reliable algorithms and detailed air shower simulations are needed. By comparing the predictions from simulation with measurements one can draw conclusions on the primary mass composition of the arriving particles.

Again predictions from simulations suffer from systematic uncertainties mainly due to statistical fluctuations involved in large-scale experiments and due to modeling of HE interactions. While the electro-weak interaction processes are reasonably well understood; above the attained energy by the man-made accelerator, modeling of hadronic multi-particle production is subject to large theoretical uncertainties. Estimation of these uncertainties are further difficult task.

Different hadronic interaction models predict different lateral shapes and different number of particles at observation level. Hence, it is possible to test and compare the available interaction models by studying these EAS parameters. Moreover, some of these parameters like the muon content, depth of shower maximum X_{max} , the expected lateral shape etc. also depend on the mass of primary cosmic rays. Heavier primaries lead, on average, to a flatter

C. C. Thakuria is with the Department of Physics, Tihu College, Tihu, Nalbari, Assam, INDIA. Phone: +91 94350 15996, e-mail: chabin27@yahoo.com

K. Boruah is Professor in the Department of Physics, Gauhati University, Guwahati, INDIA. Phone: +91 94355 43920, e-mail: kalyaneeboruah@gmail.com

distribution and lower value of X_{max} and more muons.

II. EPOS 1.99 AND QGSJET II-03

Interaction models, like DPMJET [1], EPOS [2], [3], QGSJET [4], or SIBYLL [5], [6], which are designed to treat general inelastic hadronic collisions, are developed in the framework of the Reggeon Field Theory (RFT) [7], [8], which allows one to take into consideration contributions from both "soft" and "hard" parton dynamics to the interaction mechanism. Soft non-perturbative interactions are described as soft Pomeron exchanges and dominate hadronic collisions at large impact parameters, thus giving important contributions to total, inelastic, and diffractive hadron-nucleus (nucleus-nucleus) cross sections. On the other hand, at sufficiently high energies the role of so-called semi-hard hadronic collisions which involve partons of moderately large virtualities is significantly enhanced, the smallness of the corresponding strong coupling being compensated by large collinear and infra-red logarithms and by high density of small x partons [9].

EPOS [2] is a newly developed model emerging from VENUS [10] and NEXUS models [11]. EPOS is a parton model, with many binary parton-parton interactions, each one creating a parton ladder. EPOS is a consistent quantum mechanical multiple scattering approach based on partons and strings, where cross sections and the particle production are calculated consistently, taking into account energy conservation in both cases (unlike other models where energy conservation is not considered for cross section calculations) [12]. In EPOS 1.99 reduction of the proton-nucleus cross section is done for better correlation between the number of muons and the number of electrons at ground based air shower measurement. [13], [14]

QGSJET II-03 [16], [17]: QGSJET [4], originally based on the Quark-Gluon String model picture of high energy interactions, treats hadronic and nuclear collisions in the framework of Gribov's reggeon approach [7], [8]. It has been generalized to treat nucleus-nucleus interactions and semi-hard processes using the so-called "semi-hard Pomeron" approach. The semi-hard processes are described by so-called enhanced Pomeron diagrams and proved to be of extreme importance for a correct treatment of very high energy hadronic interactions [15]. QGSJET scheme is based on the assumption that individual parton cascades, described as Pomeron exchanges, proceed independently of each other which is not true at high energy regime. At high energies parton cascades strongly overlap and interact with each other. These effects are described as Pomeron-Pomeron interactions. A new hadronic interaction model QGSJET-II-3 has been developed including the

treatment of this non-linear interaction effects. QGSJET II-03 is based on the assumption that corresponding effects are dominated by “soft (low momentum transfer) partonic processes. Essential enhanced contributions have been resummed to all orders, both for so-called uncut (elastic scattering) diagrams and for various unitarity cuts of those diagrams, corresponding to particular final states of the interaction. QGSJET II-03 is based on the obtained solutions, explicitly treating the corresponding effects in individual hadronic (nuclear) collisions [16], [17].

A. FLUKA 2011

In CORSIKA [18], [19] apart from seven high energy interaction models there are three low energy models, namely GHEISHA [20], UrQMD [21], and FLUKA [22]. The Fluka hadron-nucleon interaction models are based on resonance production and decay below a few GeV , and on the Dual Parton model above. Two models are used also in hadron-nucleus interactions [23], [24].

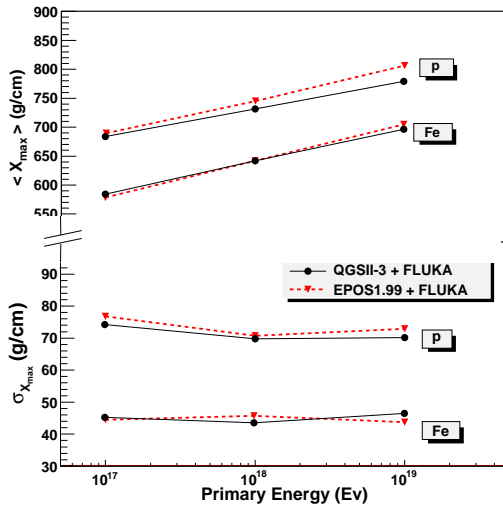


Fig. 1

AVERAGE X_{max} VS LOG OF PRIMARY ENERGY (TOP) $\sigma_{X_{max}}$ VS LOG OF PRIMARY ENERGY (BOTTOM)

B. Muon Number

Muons are produced mainly by decay of charged pions and kaons in a wide energy range. Usually they are not produced directly on the shower axis. Multiple Coulomb scattering in the atmosphere and in the detector shielding may change the muon direction. It is known that the reconstruction of the longitudinal development of the muon component provides a powerful tool for primary mass measurement, giving an information similar to that obtained with the fluorescence technique, but in the energy range not accessible by the detection of fluorescence light. In

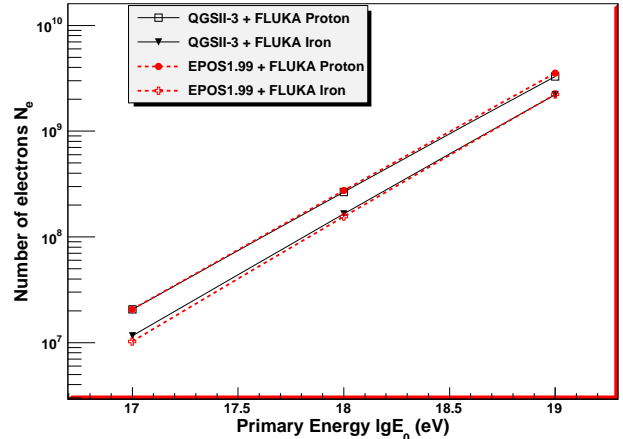


Fig. 2
AVERAGE ELECTRON SHOWER SIZE VS LOG OF PRIMARY ENERGY

some experiment like KASCADE truncated muon size is calculated by integrating muons between $40m$ and $200m$. Instead of total number of muons, truncated muon size is considered for EAS study [25]. The range of muon truncation is from $140m$ - $360m$ in KASCADE Grande.

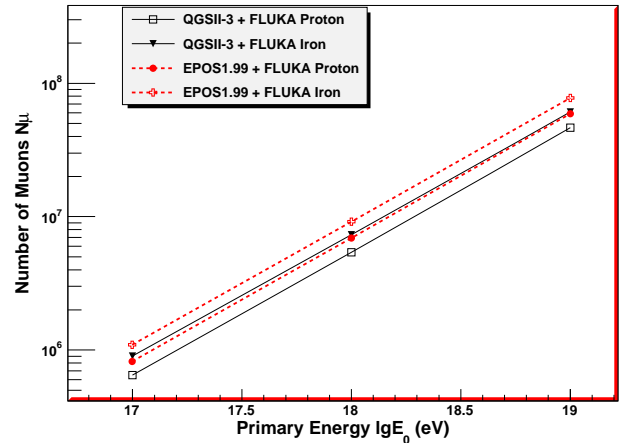


Fig. 3
AVERAGE MUON NUMBER VS LOG OF PRIMARY ENERGY

C. Depth of Shower max

The depth of shower maximum contains information about the mass of the primary CR initiating the shower as well as about the properties of hadronic interactions. The average value X_{max} depends on the primary energy E and on the number of nucleons A :

$$X_{max} = \alpha (\ln E - \ln A) + \beta \quad (1)$$

with α and β depending on the the details of hadronic interactions. Their values are very sensitive to changes in cross-section, multiplicity and elasticity [26]. Eq.1 is derived from a simple generalization of the Heitler model

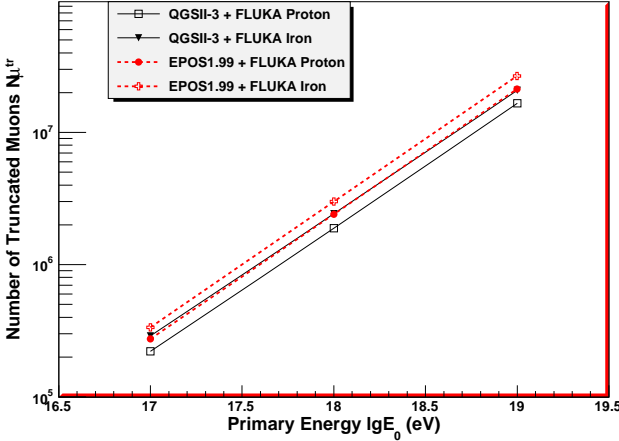


Fig. 4

AVERAGE TRUNCATED MUON NUMBER VS LOG OF PRIMARY ENERGY

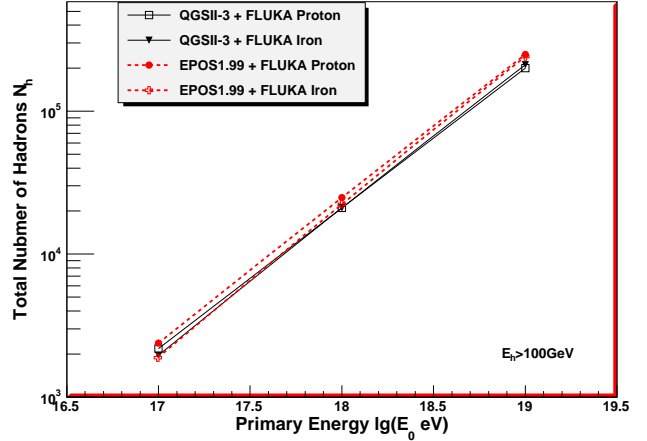


Fig. 5

HADRON NO VS LOG OF PRIMARY ENERGY

TABLE I

SLOPE OF X_{max} AND INTERCEPT

Model & Primary	Slope of X_{max}		Intercept	
	α	error	β	error
<i>EPOS</i> - <i>p</i>	58.3690	± 1.64891	-303.488	± 29.7108
<i>QGSII</i> - <i>p</i>	47.5875	± 0.24876	-125.219	± 4.48227
<i>EPOS</i> - <i>Fe</i>	62.9539	± 1.55497	-491.491	± 28.0169
<i>QGSII</i> - <i>Fe</i>	55.2977	± 0.23593	-354.504	± 4.25079

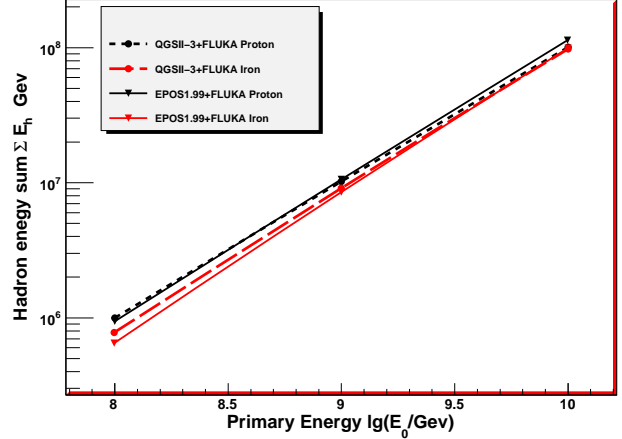
to showers induced by hadronic primaries, but it provides a good description of the X_{max} evolution predicted by hadronic models currently in use. In some specific energy range, α and β may be considered independent of E . Another sensitive parameter is $\sigma_{x_{max}}$, expressing quantitatively the shower to shower fluctuations of X_{max} . It depends mainly on the cross section and less strongly on the elasticity. This makes fluctuations in X_{max} , a good parameter to study hadronic cross sections at ultra-high energies.[27]

III. SIMULATION

The shower simulations are performed using CORSIKA-6990 [28]. Hadronic interactions at low energies($E < 80$ GeV) are modelled using the FLUKA-2011 code. High Energy interactions are treated with EPOS 1.99 and QGSJET II-3. Vertical showers initiated by primary protons and iron nuclei are simulated. Observation level is taken at the sea level, US standard atmosphere taking default magnetic field in CORSIKA. 1000 showers are simulated each for three primary energies 10^{17} , 10^{18} & 10^{19} eV, two primary mass(p & Fe) and for two HE models EPOS 1.99 and QGSJET II-3. All together 12,000 showers are generated.

IV. RESULTS

The Depth of maximum X_{max} , and the RMS value $\sigma_{x_{max}}$ for the two models are plotted as function of en-

Fig. 6
HADRON ENERGY SUM VS LOG OF PRIMARY ENERGY

ergy in Figures 1. It is seen that heavier primary produces shower maximum at lower depth with lower fluctuation compared with lighter primary as expected. The average total number of electrons(N_e), muons(N_μ), truncated muons(N_μ^{tr}), hadrons ($E_h > 100$ GeV), and sum of energies of all the hadrons($E_h > 100$ GeV) registered at the ground level for the interaction models EPOS 1.99 and QGSJET II-03 are plotted as a function of energy in Figures 2, 3, 4, 5, and 6 respectively.

It is seen that, both models yield a linear dependence of these components with energy in Log-Log scale.

A. Dependence of X_{max} with primary Energy

The value of X_{max} and also the slope of the curve for proton primary for EPOS 1.99 is slightly higher than that of QGSJET II-03. Again, for iron primary also the slope of the curve has higher value for EPOS 1.99, while the values of X_{max} are nearly equal for both the models. The value of $\sigma_{x_{max}}$ for proton primary for EPOS 1.99 is slightly

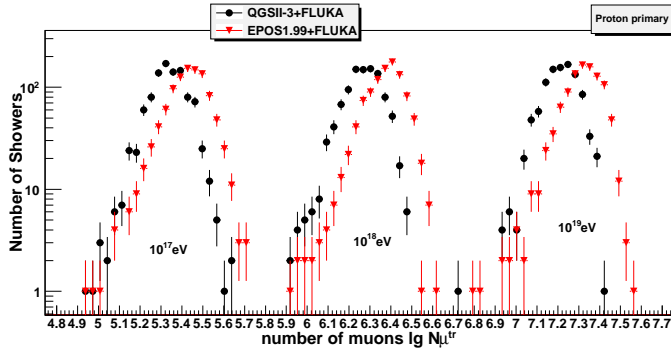


Fig. 7

DISTRIBUTION OF THE NUMBER OF TRUNCATED MUONS FOR PROTON PRIMARY

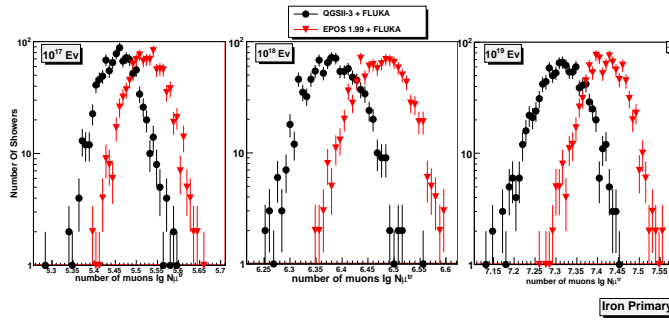


Fig. 8

DISTRIBUTION OF THE NUMBER OF TRUNCATED MUONS FOR IRON PRIMARY

higher (average about 3% high) than that of QGSJET II-03. But for iron primary there is no such trend observed. The fitted values of the slope α and intercept β are given in the Table I.

B. Primary Energy Correlations

From Figures 2 through 6, it is seen that, there is no significant differences in the electron shower size and sum of hadron energy for the two models considered in the chosen primary energies for proton and iron primaries. However for muons (Fig. 3, 4) differences between the predictions of the two models are significant. The number of muons is larger for EPOS1.99 model as compared to QGSJET II-03 for both the primaries. From the figure 3, it is seen that there is very little overlap in the region bounded by p & Fe primaries for two models considered. However, for truncated muons (in the range 40m-200m) there is no overlap beyond 10^{18} eV (Figure 4). For $E_h > 100\text{GeV}$ hadrons, total number for both proton & iron primaries are found to be significantly more for EPOS than that for QGSJET II-03 (Figure 5). However, considering the sum total of energies of all the hadrons ($E_h > 100\text{GeV}$), there is no significant difference between the two models (Figure 6).

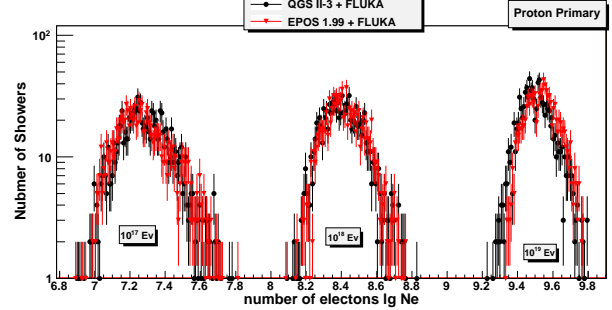


Fig. 9

DISTRIBUTION OF THE NUMBER OF ELECTRONS FOR PROTON PRIMARY

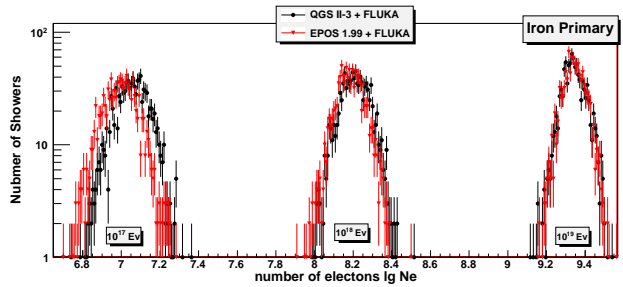


Fig. 10

DISTRIBUTION OF THE NUMBER OF ELECTRONS FOR IRON PRIMARY

cated muons (in the range 40m-200m) there is no overlap beyond 10^{18} eV (Figure 4). For $E_h > 100\text{GeV}$ hadrons, total number for both proton & iron primaries are found to be significantly more for EPOS than that for QGSJET II-03 (Figure 5). However, considering the sum total of energies of all the hadrons ($E_h > 100\text{GeV}$), there is no significant difference between the two models (Figure 6).

C. Distribution of truncated muon numbers and electron numbers

Distributions of truncated muon numbers $lg(N_\mu^{tr})$ for proton and iron primaries are plotted in Figure 7 and 8. It is seen that EPOS1.99 yields higher value of $lg(N_\mu^{tr})$ than QGSJET II-03. The mean & s.d. of these distributions are tabulated in Table II, and significance test done (C).

Distributions of electron numbers $lg(N_e)$ for proton and iron primaries are plotted in Figure 9 and 10. It is seen that EPOS1.99 produces slightly less numbers of electrons for energy 10^{17} eV for iron primary, but at 10^{19} eV, EPOS1.99 produces slightly more electrons as tabulated in Table III,

TABLE II
AVERAGE TRUNCATED MUON NUMBER AND RMS VALUE

Energy/Model (eV)	Proton Primary		Iron Primary	
	$\langle lg(N_\mu^{tr}) \rangle$	RMS	$\langle lg(N_\mu^{tr}) \rangle$	RMS
$10^{17} - QGSII$	5.33582	0.09227	5.45870	0.04113
$10^{17} - EPOS$	5.42664	0.10664	5.52427	0.04210
$10^{18} - QGSII$	6.26616	0.09035	6.38253	0.04637
$10^{18} - EPOS$	6.37158	0.09563	6.47433	0.04434
$10^{19} - QGSII$	7.21209	0.08441	7.31510	0.05116
$10^{19} - EPOS$	7.31632	0.09665	7.41770	0.04526

TABLE III
AVERAGE ELECTRON NUMBER AND RMS VALUE

Energy/Model (eV)	Proton Primary		Iron Primary	
	$\langle lg(N_e) \rangle$	RMS	$\langle lg(N_e) \rangle$	RMS
$10^{17} - QGSII$	7.28989	0.14648	7.05567	0.08888
$10^{17} - EPOS$	7.27924	0.15111	6.99535	0.09171
$10^{18} - QGSII$	8.40937	0.11724	8.21039	0.07825
$10^{18} - EPOS$	8.42408	0.11274	8.18449	0.07497
$10^{19} - QGSII$	9.50743	0.09597	9.34173	0.06344
$10^{19} - EPOS$	9.54035	0.08953	9.34330	0.06105

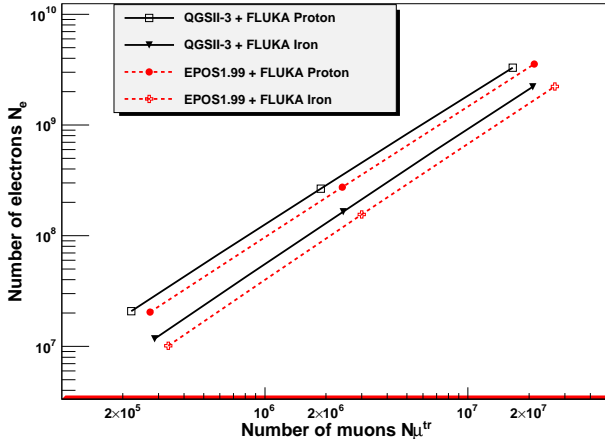


Fig. 11

NUMBER OF ELECTRONS VS NUMBER OF TRUNCATED MUONS

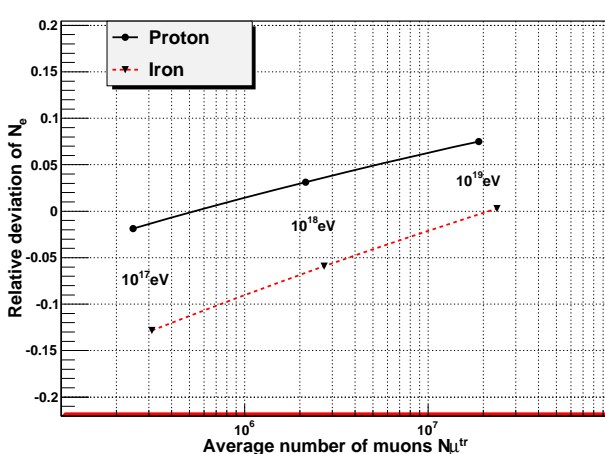


Fig. 12

RELATIVE DEVIATION OF THE NUMBER OF ELECTRONS VS AVERAGE NUMBER OF TRUNCATED MUONS

and significance test done(C).

D. Electron to muon correlation

The average number of electrons as a function of the number of truncated muons are plotted in figure 11 for the two models. Slopes of all the curves are almost equal. To emphasize the differences between the model predictions, relative deviation in the model prediction EPOS1.99 with respect to the QGSJET II-3 prediction, $(N_e^{EPOS} - N_e^{QGS})/N_e^{QGS}$ is plotted against the mean of N_μ^{QGS} and N_μ^{EPOS} in Figure 12. It is seen that for proton primary, EPOS1.99 predicts slightly less (about 2%) electrons for $10^{17}eV$ proton-induced showers, slightly more (about 3%) electrons for $10^{18}eV$ and about 8% more electrons for $10^{19}eV$ primary energy. But for iron primary at $10^{17}eV$, $10^{18}eV$, and, $10^{19}eV$, EPOS 1.99 yields about 12% lesser, about 6% lesser and nearly equal (difference

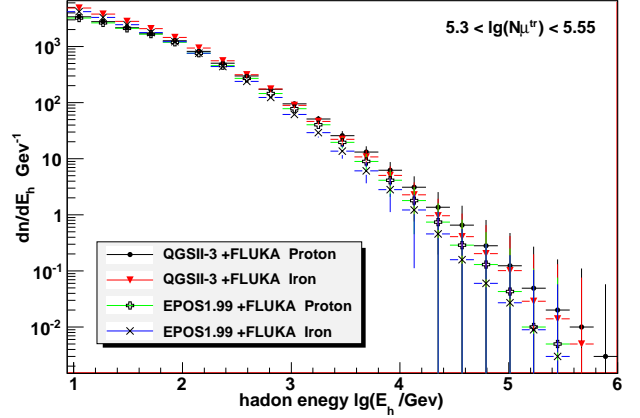


Fig. 13

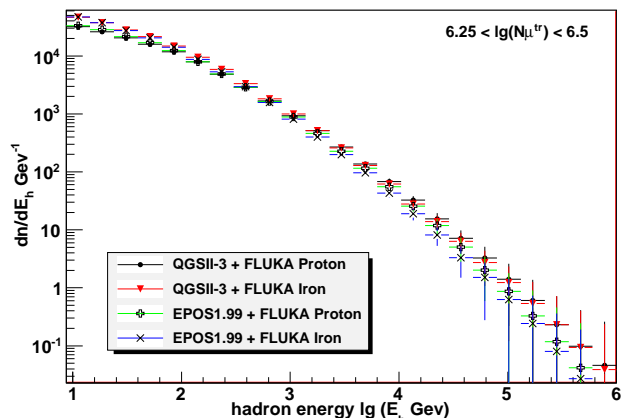
HADRON ENERGY DISTRIBUTION ($10^{17}eV$)

Fig. 14

HADRON ENERGY DISTRIBUTION ($10^{18}eV$)

is less than 1%) numbers of electrons as compared with QGSJET II-3 predictions.

E. Variation in hadron component

Total average number hadrons with energy $E_h > 100GeV$, for both primary masses & at all the three energies show significant difference between the two models (D). Energy spectrum of registered hadrons for $10^{17}eV$, $10^{18}eV$, and $10^{19}eV$ primary for both the models considered are displayed in the Figures 13, 14, and 15 respectively. There are apparently no distinguishable differences. All the four data plots are overlapped to each-other with their error-bars.

V. SUMMARY

Although X_{max} , shower size, hadron energy sum, hadron energy distribution shows no significant difference between the two HE models EPOS 1.99 (FLUKA) and QGSJET II-3 (FLUKA); muon number, hence electron to muon correlation shows incompatibility between them.

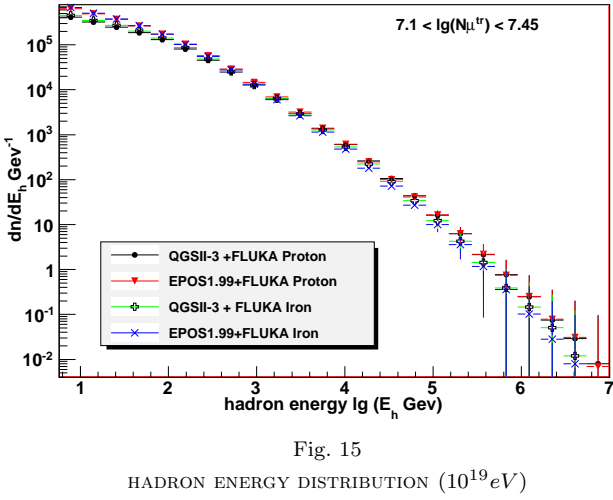


Fig. 15

HADRON ENERGY DISTRIBUTION ($10^{19} eV$)

EPOS 1.99 (FLUKA) predicts more muons than QGSJET II-3 (FLUKA). Also hadron($E_h > 100 GeV$) shower size prediction by EPOS 1.99 (FLUKA) yields higher values irrespective of primaries considered as compared to that by QGSJET II-3 (FLUKA). Modifications may be needed for one, or, both of the models considered herein by comparing the model predictions with experimental data.

VI. ACKNOWLEDGEMENTS

The authors thankfully acknowledge UGC for computational infrastructure support under SAP. and C. C. Thakuria acknowledges UGC for fellowship under FDP.

REFERENCES

- [1] J. Ranft, *Phys. Rev. D* **51** (1995) 64; preprint [hep-ph/9911213](http://arxiv.org/abs/hep-ph/9911213) (1999)
- [2] K. Werner, F. M. Liu and T. Pierog, *Phys. Rev. C* **74** (2006) 044902
- [3] K. Werner, and T. Pierog, [arXiv:0707.3330v1\[astro-ph\]](http://arxiv.org/abs/0707.3330v1).
- [4] N.N. Kalmykov, S.S. Ostapchenko, and A.I. Pavlov, *Nucl. Phys. B (Proc. Suppl.)* **52B** (1997) 17
- [5] R.S. Fletcher, T.K. Gaisser, P. Lipari, and T. Stanev, *Phys. Rev. D* **50** (1994) 5710; J. Engel, T.K. Gaisser, P. Lipari, and T. Stanev, *Phys. Rev. D* **46** (1992) 5013
- [6] R. Engel, T.K. Gaisser, P. Lipari, and T. Stanev, *Proc. 26th Int. Cosmic Ray Conf.*, Salt Lake City (USA), **1** (1999) 415; E.-J. Ahn, R. Engel, T.K. Gaisser, P. Lipari, and T. Stanev, *Phys. Rev. D* **80** (2009) 094003
- [7] V.N. Gribov, *Sov. Phys. JETP* **26** (1968) pp-414.
- [8] V.N. Gribov, *Sov. Phys. JETP* **29** (1969) pp-483.
- [9] S. Ostapchenko (preprint [arXiv:1010.1869v2](http://arxiv.org/abs/1010.1869v2))
- [10] K. Werner, *Phys. Rep.* **232** (1993) 87
- [11] H.J. Drescher, M. Hladik, S. Ostapchenko, T. Pierog, and K. Werner, *Phys. Rep.* **350** (2001) 93 (preprint [hep-ph/0007198](http://arxiv.org/abs/hep-ph/0007198) (2000))
- [12] M. Hladik, H. J. Drescher, S. Ostapchenko, T. Pierog, and K. Werner *et al.*, *Phys. Rev. Lett.* **86**, 3506 (2001), [arXiv:hep-ph/0102194](http://arxiv.org/abs/hep-ph/0102194).
- [13] T. Pierog, Iu. Karpenko, S. Porteboeuf, and K. Werner, [arXiv:1011.3748v1\[astro-ph.HE\]](http://arxiv.org/abs/1011.3748v1).
- [14] K. Werner, and T. Pierog, Proc. 31st ICRC, ODZ 2009
- [15] S. Ostapchenko (preprint [arXiv:hep-ph/0412332](http://arxiv.org/abs/hep-ph/0412332))
- [16] S.S. Ostapchenko, *Nucl. Phys. B (Proc. Suppl.)* **151** (2006) 143-147; *Phys. Rev. D* **74** (2006) 014026
- [17] S. Ostapchenko *AIP Conf. Proc.* **928** (2007) pp-118.
- [18] J.N. Capdevielle *et al.*, Report **KfK 4998** (1992), Kernforschungszentrum Karlsruhe
- [19] D. Heck and J. Knapp, Report **FZKA 6097** (1998), Forschungszentrum Karlsruhe; available from <http://www-ik.fzk.de/~heck/publications/>
- [20] H. Fesefeldt, Report **PITHA-85/02** (1985), RWTH Aachen
- [21] S.A. Bass *et al.*, *Prog. Part. Nucl. Phys.* **41** (1998) 225; M. Bleicher *et al.*, *J. Phys. G: Nucl. Part. Phys.* **25** (1999) 1859; <http://urqmd.org/>
- [22] A. Fassò, A. Ferrari, S. Roesler, P.R. Sala, G. Battistoni, F. Cerutti, E. Gadioli, M.V. Garzelli, F. Ballarini, O. Ottolenghi, A. Empl and J. Ranft, *The physics models of FLUKA: status and recent developments*, Computing in High Energy and Nuclear Physics 2003 Conference (CHEP2003), La Jolla, CA (USA), March 24-28, 2003 (paper MOMT005); eConf C0303241 (2003); arXiv:hep-ph/0306267; <http://www.fluka.org/references.html>
- [23] A. Ferrari, P.R. Sala, A. Fassò, and J. Ranft, FLUKA: a multi-particle transport code, CERN-2005-10 (2005), INFN/TC 05/11, SLAC-R-773.
- [24] G. Battistoni, S. Muraro, P.R. Sala, F. Cerutti, A. Ferrari, S. Roesler, A. Fassò, J. Ranft, The FLUKA code: Description and benchmarking, Proceedings of the Hadronic Shower Simulation Workshop 2006, Fermilab 68 September 2006, M. Albrow, R. Raja eds., AIP Conference Proceeding 896, 31-49, (2007)
- [25] T. Antoni *et al.* *NuclInstr and Meth A* **513**, pp 490-510 (2003)
- [26] R. Ulrich, *Phys. Rev. D* **83**, 054026 (2011).
- [27] Ralf Ulrich, *Phys. Rev. D.* **83**, 054026 (2011)
- [28] D. Heck, J. Knapp, J.N. Capdevielle, G. Schatz, and T. Thouw, Report **FZKA 6019** (1998), Forschungszentrum Karlsruhe; available from http://www-ik.fzk.de/corsika/physics_description/corsika_phys.html

APPENDIX

A. STATISTICAL TEST

A. Z-test results for X_{max} distribution (Table IV)

The null hypothesis is

H_0 =There is no difference between the two samples (QGSJET II-03 data and EPOS1.99 data).

TABLE IV

Z STATISTICS FOR X_{max}

Energy/Primary (eV)	$X_{max} \text{ Dist}^n$	
	Z	Inference
$10^{17} - \text{Proton}$	1.81	Not Significant
$10^{17} - \text{Iron}$	3.00	Moderately Significant
$10^{18} - \text{Proton}$	4.41	Significant
$10^{18} - \text{Iron}$	0.28	Not Significant
$10^{19} - \text{Proton}$	8.65	Highly Significant
$10^{19} - \text{Iron}$	3.83	Moderately Significant

B. Z-test results for α and β (Table V)

The null hypothesis is

H_0 =There is no difference between the parameters for QGSJET II-03 and EPOS1.99 .

TABLE V

Z STATISTICS FOR α AND β

Parameter & Primary	α and β	
	Z	Inference
$\alpha - \text{Proton}$	6.466	Significant
$\alpha - \text{Iron}$	4.981	Significant
$\beta - \text{Proton}$	5.933	Significant
$\beta - \text{Iron}$	4.834	Significant

It is seen that the parameters α and β describing X_{max} (Equation 1), show significant differences for EPOS and QGSJET II, irrespective of the primaries.

C. Z-test results for N_μ^{tr} and N_e distributions (Table VI)

The null hypothesis is
 H_0 =There is no difference between the two samples (QGSJET II-03 data and EPOS1.99 data).

TABLE VI
Z STATISTICS FOR N_μ^{tr} AND N_e DISTⁿS

Energy/Primary (eV)	N_μ^{tr} Dist ⁿ		N_e Dist ⁿ	
	Z	Inference	Z	Inference
$10^{17} - Proton$	20.36	Highly Significant	1.60	Not Significant
$10^{17} - Iron$	35.22	Highly Significant	14.93	Highly Significant
$10^{18} - Proton$	25.34	Highly Significant	2.86	Moderately Significant
$10^{18} - Iron$	45.25	Highly Significant	7.56	Significant
$10^{19} - Proton$	25.68	Highly Significant	7.93	Significant
$10^{19} - Iron$	47.50	Highly Significant	0.56	Not Significant

Average truncated muon number shows highly significant difference between the two models. For the average electron number, for lower energy($10^{17}eV$) high significance for iron primary, but no significant difference for proton primary is seen, whereas at higher energy($10^{19}eV$), no significance for iron, but significant differences for proton primary is observed (Table VI).

D. Z-test results for total hadron number ($E_h > 100GeV$) (Table VII)

The null hypothesis is
 H_0 =There is no difference between the two samples (QGSJET II-03 data and EPOS1.99 data).

TABLE VII
Z STATISTICS FOR TOTAL HADRON NUMBER ($E_h > 100GeV$)

Energy/Primary (eV)	N_h Dist ⁿ	
	Z	Inference
$10^{17} - Proton$	4.07	Significant
$10^{17} - Iron$	21.09	Highly Significant
$10^{18} - Proton$	8.91	Highly Significant
$10^{18} - Iron$	6.52	Highly Significant
$10^{19} - Proton$	13.25	Highly Significant
$10^{19} - Iron$	15.59	Highly Significant